Chemical Physics Letters 591 (2014) 197–202

Contents lists available at ScienceDirect

Chemical Physics Letters

journal homepage: www.elsevier.com/locate/cplett

Three-dimensional networks of hydrogen bonds in periodic arrays of molecular modules containing amide-(ethylene glycol) and amide-(ethylene glycol)-amide: *Ab initio* picture

L. Malysheva [a,b,*], O. Kapitanchuk [a], A. Onipko [b,*]

[a] Bogolyubov Institute for Theoretical Physics, 03680 Kyiv, Ukraine
[b] Laboratory on Quantum Theory in Linköping, ISIR, Box 8017, S-580 08 Linköping, Sweden

ARTICLE INFO

Article history:
Received 20 August 2013
In final form 14 November 2013
Available online 21 November 2013

ABSTRACT

First-principle modeling is used to identify the most likely conformations of two molecular modules $A(EG)_{3,6}$ and $A(EG)_{3,6}CH_2A$ (A = CONH, EG = $(CH_2)_2O$), which in self-assembled monolayers form, respectively, one- and two-layered networks of hydrogen-bonded amides (HBAs). The molecular bond lengths and angles within HBA chains, which are formed within $(\sqrt{3}\times\sqrt{3})$ R30° hexagonal arrays of identical modules, were calculated by exploiting the DFT/BP86/6-31G method. The results from our first-principle conformation analysis highlight an integrated picture of hydrogen bonding in related families of assemblies containing one and two amide groups per molecule, e.g., in HS–$(CH_2)_n$A$(EG)_m$H and HS–$(CH_2)_n$A$(EG)_m$$CH_2$A–$(CH_2)_l$H SAMs on gold.

1. Introduction

Oligo(ethylene glycol)-containing self-assembled monolayers (SAMs) on metal and isolating substrates have become a useful tool in a variety of biotechnological/analytical and biomedical applications [1–4]. The fabrication of bio-interfaces with desired properties (e.g., those rendering them resistant against protein absorption [5–8] and/or favoring tethering for specific binding of proteins [9–11] and DNA [12]) require fundamental understanding of self-assembly mechanisms, phase behavior, stability factors, and interactions between different layers within complex self-assemblies. In the pioneering [5,6] and subsequent studies on SAM protein resistance [7–11], the oligo(ethylene glycol) (OEG) component $(EG)_n$ (EG≡$(CH_2)_2O$) was linked to alkanethiol spacer HS—$(CH_2)_n$ ≡HS—C_n via oxygen (ether). Due to replacement of ether by an amide group, HS–C_mO$(EG)_n$H → HS–C_mA$(EG)_n$H, crystallinity (especially important for molecules with alkanethiol spacers), reproducibility, and stability of OEG containing SAMs have been significantly improved [13–15]. The stabilizing and ordering effects of amides buried in alkanethiol SAMs were first noticed by Clegg and Hatchison [16]. They were attributed to the lateral hydrogen bonding between neighboring amide groups that improves the two-dimensional, crystal-like structure of alkanethiol-based self-assembled monolayers, see Refs. [16–24] and references therein. It was also demonstrated that an increased number of amide groups per SAM constituent results in forming a three dimensional network of hydrogen bonds and hence, in even more considerable improvements of SAM structure [18].

Following this route, the stabilizing ability of additional amide bridges has been used to synthesize SAMs by chaining C_m, A, and $(EG)_n$ building blocks [25–27]. The new family of self assemblies of molecules HS–C_{15}A$(EG)_6C_1$A–C_mH, m = 1, 2, 8, 9, and 16 was shown to possess an increased thermal stability and much stronger and sharper features in the infrared reflection absorption (IR RA) spectra as compared to the more conventional OEG-terminated SAMs which have one amide group per constituent [13–15]. Noteworthy, even samples with a very short upper alkyl layer m = 1 exhibited crystalline-like IR RA spectra. This observation strongly supports the formation of additional 'stabilizing' hydrogen bonds between the upper amide groups.

Heretofore, the hydrogen bonding networks observed in a variety of SAMs was mostly addressed in experimental studies. Recent and probably the only first-principle modeling of monolayers stabilized by buried amides describes a hexagonal periodic array of HS–C_3A$(EG)_3$H molecules (**h**, see Scheme 1) [28]. The *ab initio* optimized geometry of this structure has revealed typical changes of the amide-related dihedrals, partial reorientation of alkyl and OEG units within related SAMs [13–15] and a ~0.6 Å reduction in H···O distance, compared to the value obtained for the initial array of non-interacting molecules.

In a sense, the above mentioned results have allowed us to address the experiments on SAMs containing $A(EG)_6C_1A$ modules [27]. By using an optimized geometry of HS–C_{15}A$(EG)_6C_1$A–C_mH molecule and steric considerations we have come to the conclusion

* Corresponding authors at: Bogolyubov Institute for Theoretical Physics, 03680 Kyiv, Ukraine.
E-mail addresses: malysh@bitp.kiev.ua, mally@ifm.liu.se (L. Malysheva), aleon@lqtl.org (A. Onipko).

0009-2614/$ - see front matter © 2013 Elsevier B.V. All rights reserved.
http://dx.doi.org/10.1016/j.cplett.2013.11.031

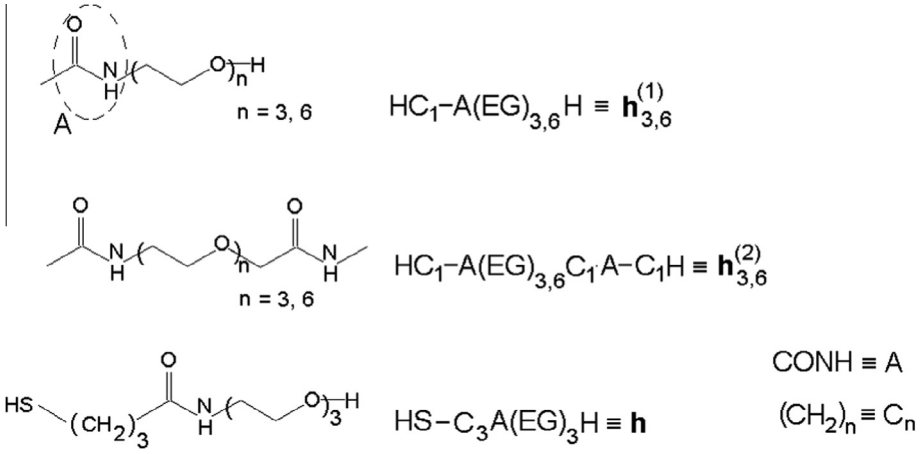

Scheme 1. The notations for investigated molecules used in the text and figures.

that a three-dimensional hydrogen bonding in the related SAMs should consist of *parallel* chains of hydrogen bonded amides (HBAs). The formation of such chains is possible due to the lower and upper amide groups which are close to parallel. However, no experimentally sound parameters of HBA chains could actually be predicted at that level of modeling. All the more so, no conclusions could be made regarding hydrogen bonding of $A(EG)_nC_1A$ modules with the length other than $n = 6$. Thus, the understanding of the microscopic structure of hydrogen bonding leaves much to be desired.

Varying the length of the SAM molecular constituents, in particular the OEG length provides an Å-precision in positioning of chemical groups across SAM interfaces. Depending on the particular purpose, the use of either shorter or longer OEG portions may be of advantage. For instance, tri(ethylene glycol) thiol derivatives with a short alkyl spacer have been used as a bio-inert molecular 'resist' for scanning probe nanolithography on gold [29]. Monolayers of longer OEGs without alkyls were used for quartz crystal microbalance with dissipation monitoring (QCM-D) sensing [30].

Keeping in mind aforementioned, we have undertaken a comparative *ab initio* study of one- and two-layered hydrogen bonding networks within hexagonal periodic arrays comprised of molecules $HC_1–A(EG)_{3,6}H$ ($\mathbf{h}^{(1)}_{3,6}$) and $HC_1–A(EG)_{3,6}C_1A–C_1H$ ($\mathbf{h}^{(2)}_{3,6}$), where the OEG portion adopts the helical conformation (Figures 1 and 2). This modeling enabled us to trace the effect of hydrogen bonding on the structure and orientation of amide and OEG units, and to specify parameters of hydrogen bonded amides within the OEG-terminated amide-bridged SAMs. To shed some light on the role of the supporting alkyl layer, the structure of array $\mathbf{h}^{(1)}_3$ is compared with already reported [28] and new data obtained for array **h**.

2. Calculation essentials

Various computation methods are used to study organic SAMs at the microscopic level. In particular, these are molecular mechanics/dynamics methods [31,32], Monte Carlo [33], and *ab initio* methods [23,24,26–28,34]. Unlike the force field description which is based on the experimental data and/or *ab initio* calculations for the corresponding class of molecules, DFT gives the sufficiently accurate reproduction of SAM interior from the first principle and at reasonable computational effort. All calculations in the present work were carried out by using the DFT methods with the help of the Gaussian 03 and Gaussian 09 sets of codes. The basis set 6-31G and the combination of Becke-exchange- and Perdew 86 correlation functional (BP86) were exploited as the main tool. Optimization of model SAMs was performed for the molecular arrays subjected to the periodic boundary conditions (PBC).

There is a considerable controversy in theoretical predictions regarding the exact position of sulfur adsorption sites within SAMs [1,35]. However, it is certainly reasonable to assume that they form a $(\sqrt{3} \times \sqrt{3})$ R30° hexagonal lattice and that the 5 Å distance between the nearest neighbor S atoms is kept fixed by the supporting Au (111) surface. Therefore, the hexagonal structure of model SAMs seems to be most appropriate for a zero-order description of lateral hydrogen bonding network in real SAMs. The optimization of two dimensional periodic array geometries was thus performed with fixed translation vectors. These were chosen to be [500] and [2.54.330] (in Å). At the same time, all the bonds, bond angles, dihedral angles, as well as all orientation angles were free to change. The effects associated with adsorbate–substrate interaction within SAMs [1] are beyond of the present consideration.

The choice of initial molecular geometry and orientation is crucial for this kind of modeling. For periodic arrays **h** and $\mathbf{h}^{(1,2)}_{3,6}$ it was obtained by the replacement of $HS–C_{15}$ with $HS–C_3$ in molecule $M1 = HS–C_{15}A(EG)_6H$, and with HC_1 in molecule $M2 = HS–C_{15}A(EG)_6C_1A–C_1H$. Thereby, we preserved the values of Euler angles (θ_E, ψ_E, φ_E), which were calculated for the equilibrium geometry of these molecules. Whenever necessary, the initial-angle values were corrected to fit the required orientation of C=O and N–H bonds. According to the experimental data [19], these bonds are nearly perpendicular to *z* axis, (the substrate normal) whereas the C–N bond has an appreciable *z*-projection. This implies that no or very weak spectral signatures of the amide A and amide I vibrations at ~3300 and ~1650 cm^{-1} can be seen in the IR RA spectra (the surface selection rule). Instead, the dominating feature is the amide II band at ~1550 cm^{-1}, whereas amide III band at ~1250 cm^{-1} has a smaller but detectable intensity. We notice that in OEG containing SAMs with buried amides, the signature of amide III vibrations is masked by CH_2 twisting vibrations [13,25,26].The molecular orientation within SAMs in focus has been discussed earlier [26,34]. Based on the *ab initio* modeling of IR RA spectroscopy data for SAMs of M1 [34] and M2 [27], the tilt and rotation angles of the supporting alkyl chain are $\theta_{C_{15}} \approx 20–25°$ and $\psi_{C_{15}} \approx -60°$. Most likely, these angles do not differ much in SAMs containing one and two amide groups per molecule [27]. At the given angles $\theta_{C_{15}}$ and $\psi_{C_{15}}$, the choice of trial azimuth angle $\varphi_{C_{15}}$ was dictated by the minimal H···O distance between the hydrogen and oxygen atoms which belong to the nearest-neighbor amide groups. For an array of free-standing molecules formed by pinning sulfur atoms to the Au (111) surface, this distance falls into the range of 2.5–3 Å. The values $\theta_{C_{15}}$, $\psi_{C_{15}}$, and $\varphi_{C_{15}}$ fully determine Euler angles of OEG (θ_E, ψ_E, φ_E), amide (θ_N, ψ_N,

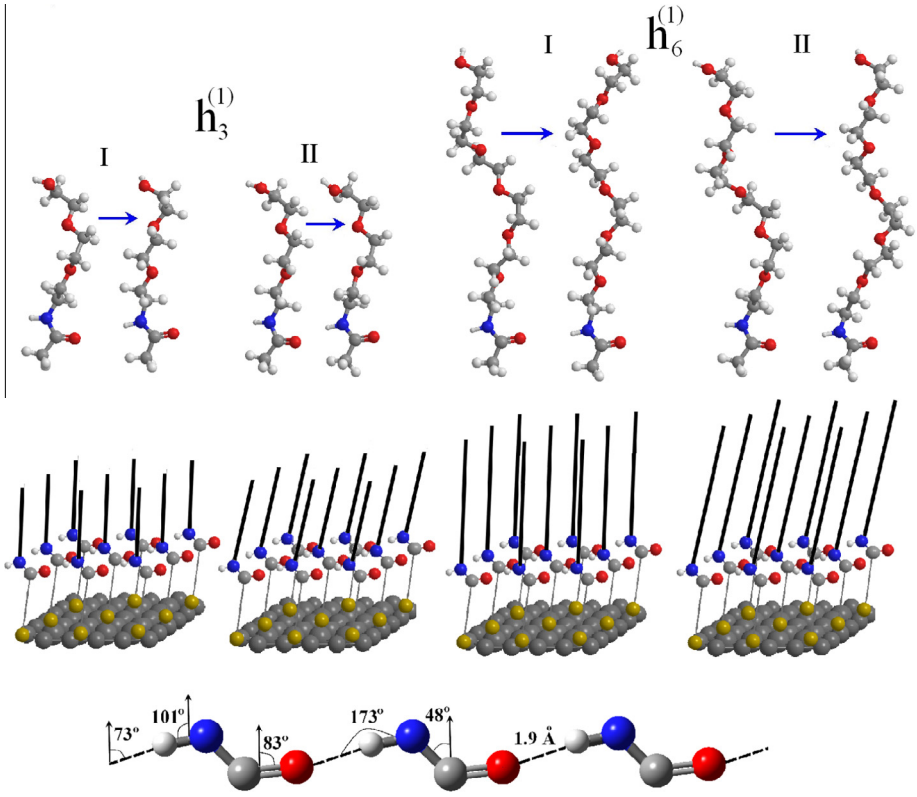

Figure 1. Upper part: molecular geometry and orientation within arrays $\mathbf{h}_{3,6}^{(1)}$ before (on the left of each pair of molecules) and after optimization. Mid part: schematic representation of the 3 × 3 fragments of the corresponding optimized arrays $\mathbf{h}_{3,6}^{(1)}$ in conformations I and II. For clarity of presentation, we explicitly show only the amide groups. Thin bars replace the groups HC_1– and are oriented along C_1–A bonds, while thick bars replace the groups –$(EG)_{3,6}$H and are oriented along OEG axis. The first C atoms in the arrays form a $(\sqrt{3} \times \sqrt{3})$ R30° lattice duplicating the S-atom lattice (dark yellow spheres). Lower part: typical characteristic angles and H···O length of hydrogen bonded amides (HBAs); these are weakly dependent on OEG length. (For interpretation of the references to colour in this figure legend, the reader is referred to the web version of this article.)

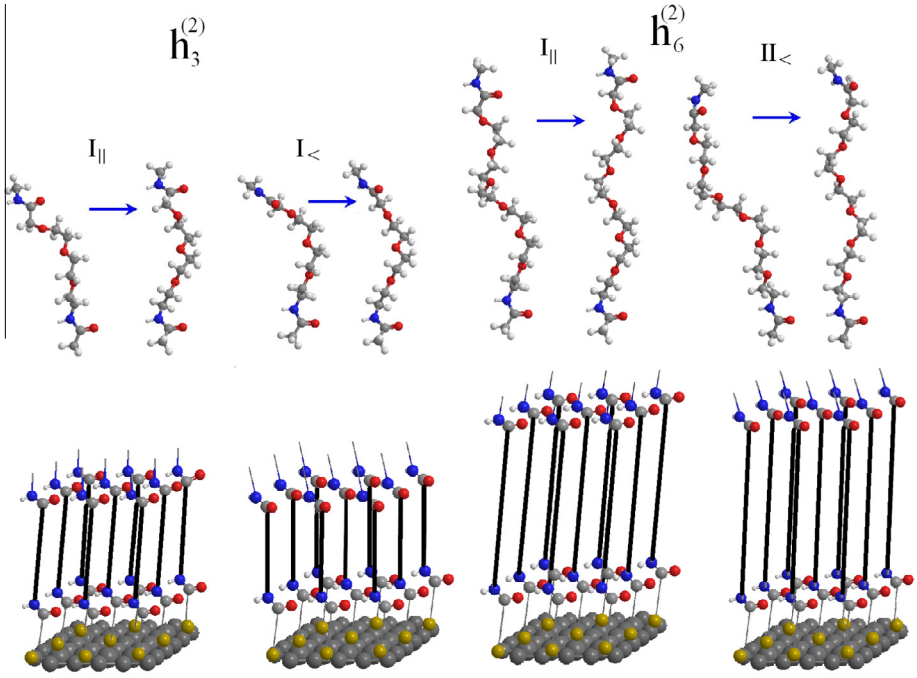

Figure 2. Same data as in Figure 1 but for arrays $\mathbf{h}_{3,6}^{(2)}$. Thick mid bars and thin uppers represent, respectively –$(EG)_{3,6}C_1$ and –C_1H; lower and upper thin bars show orientation of C_1–A and A–C1 bonds.

φ_N), as well as angles between the substrate normal z and bonds C=O ($\gamma_{C=O}$) and N–H (γ_{N-H}), Tables 1 and 2.

The optimized geometries of the arrays of molecules M1 and M2 were obtained with the help of BP86/6-31G method. In

addition, some conformations of array $\mathbf{h}_3^{(2)}$ were re-optimized with 6-31G* basis set. However, no significant difference between 6-31G and 6-31G* calculations has been revealed. To be specific, for $\mathbf{h}_3^{(2)}$ array, the maximal difference in dihedral angles is less than 3°, while the bond angles, bond lengths and parameters of HBA chains are practically the same. For $\mathbf{h}_6^{(1,2)}$ arrays, the time of calculations was substantially reduced by using the density fitting approximation [36]. The array geometry obtained in this way was re-optimized afterwards according to the standard routine. Nevertheless, this modeling (run on two PCs provided by the SI grant) turned out to be memory- and time consuming.

3. Results and discussion

As mentioned above, the best fit of molecules M2 arranged in a $(\sqrt{3}\times\sqrt{3})$ R30° hexagonal lattice implies a spacing of ~2.5–3 Å between the amide proton and the nearest-neighbor carbonyl oxygen atom. In the initial geometry of **h** array, this distance is ~2.5 Å [28]. So, the reduction to the typical H···O distance ~1.9 Å in arrays $\mathbf{h}_{3,6}^{(2)}$ requires more considerable changes of amide and OEG dihedrals than it is needed to establish hydrogen bonds in the **h** array. At first glance, such an adjustment to the equilibrium SAM geometry might even seem impossible. However, our modeling has demonstrated that (as a reflection of inherent flexibility of ethylene glycols) the multi-dimensional configuration space of SAM geometry suggests a large number of close energy minima associated with the formation of HBA chains. In other words, even a single minimum that corresponds to the equilibrium of an isolated molecule can give rise to several in-SAM molecular geometries with a large energy gain, provided the hydrogen bonding is established. Further analysis of possible array conformations has identified only two conformers of $A(EG)_6C_1A$ module as such which are likely to be realized within SAMs studied experimentally [25–27]. The forthcoming exemplifies what has been just stated.

The isolated molecules tried in this modeling have optimized conformations with a unique value of CNCC dihedral, $\tau_{CNCC}\approx -90°$. For comparison, in molecules M1 and M2, this angle equals −105° and −96°, respectively. Following the calculation scheme described above, we have arrived at array geometries with two different molecular conformations having a smaller and larger $|\tau_{CNCC}|$. More precisely, the molecules in the array environment adopt $\tau_{CNCC}\approx -80°$ in conformation I, and $\tau_{CNCC}\approx -115°$ in conformation II, Table 1. In the first trial, conformation II was obtained for arrays $\mathbf{h}_3^{(1)}$ and **h**, and conformation I – for the rest of arrays. Thereafter, the optimization was carried out for the initial geometry of arrays $\mathbf{h}_3^{(1)}$ and **h** in conformation I, and for the rest of arrays in conformation II. Similar optimization cycles were repeated many times with a variety of initial geometries.As a result, we have found that arrays $\mathbf{h}_{3,6}^{(2)}$ can adopt several conformations, distinguishable by the dihedral angle τ_{OCCN} referring to the upper amide. This angle is dependent on the OEG length and equals, according to labeling in Figure 2, $I_{||}=-205°$, $I_<=-157°$ ($\mathbf{h}_3^{(2)}$), $I_{||}=-98°$, $II_<=-99°$ ($\mathbf{h}_6^{(2)}$). These are just a few examples from a list of possible array geometries, where hydrogen bond networks have very similar parameters of HBA chains.

Some of the optimized array geometries have been classified as artifacts by the examination of characteristic dihedral angles (τ_{CNCC} and τ_{OCCN}) and Euler angles. These parameters determine the observed thickness of self assemblies of $HS–C_{15}A(EG)_6C_1A–C_nH$ molecules [27]. We have found several optimized array conformations which suggest a non-realistically small SAM thickness. These have been eliminated from further consideration.Table 1 indicates that the optimized geometries I and II with different values of dihedral angle τ_{CNCC} (lower amide) have different molecular orientations. Furthermore, the interrelation between the adopted conformational state, I or II, and the angle between the upper and lower HBA chains is not the same in arrays $\mathbf{h}_3^{(2)}$ and $\mathbf{h}_6^{(2)}$. This angle takes zero value (parallel HBA chains) when both arrays adopt conformation $I_{||}$ with nearly the same dihedral $\tau_{CNCC}=-78°$ ($\mathbf{h}_3^{(2)}$) and −79° ($\mathbf{h}_6^{(2)}$), but over 100° difference in values of dihedral τ_{OCCN}. In contrast, the array geometry with HBA chains crossed at 60° corresponds to conformation $I_<$ of array $\mathbf{h}_3^{(2)}$ ($\tau_{CNCC}=-77°$, $\tau_{OCCN}=-157°$), and to conformation $II_<$ of array $\mathbf{h}_6^{(2)}$ ($\tau_{CNCC}=-117°$, $\tau_{OCCN}=-99°$).

Table 2 and Figure 3 provide compelling proofs of the formation of hydrogen bonds which interlink $A(EG)_6C_1A$ modules and yield exhaustive information about HBA chains ···=O···H–N–C=O···H··· piercing the array in lateral direction at two levels. The lengths of hydrogen bonds of lower and upper HBA chains show small variations (actually, negligible within measurement accuracy). All other parameters of these chains are also marginally different. Angles ∠(H···O,H···O) = 15° and 65° are well seen in Figure 3, representing the top view of array $\mathbf{h}_6^{(2)}$ in conformations $I_{||}$ and $II_<$.

Comparing array $\mathbf{h}_6^{(2)}$ with $\mathbf{h}_6^{(1)}$ and $\mathbf{h}_3^{(1,2)}$, one can notice only minor differences in HBA parameters, which are weakly dependent on the adopted conformation. At the same time, the amide orientation shows a substantial dependence on the conformation state. Also, the OEG orientation depends on the adopted conformational state, OEG length, and on the presence or absence of supporting alkanethiol layer. In particular, the latter can change the CNCC dihedral angle (−79° → −104°, Table 1) resulting in a considerable reorientation of OEG chain.

Table 1
DFT optimized Euler and amide-related dihedral angles (in grades) within hexagonal periodic arrays $\mathbf{h}_{3,6}^{(1)}$, $\mathbf{h}_{3,6}^{(2)}$, and **h** in different conformational states. For a detailed definition of Euler angles see Ref. [34].

Array	θ_E, ψ_E, φ_E	θ_N, ψ_N, φ_N	τ_l	τ_u	τ_{CNCC}	τ_{OCCN}
$\mathbf{h}_6^{(2)}I_{||}$	4, 37, −129	(−49, 41, −26)/(−54, −45, 31)	80	69	−79	−98
$II_<$	11, −2, −152	(−43, −11, 9)/(−54, −45, −29)	75	70	−116	−98
$\mathbf{h}_6^{(1)}$ I	4, 32, −124	−48, 40, −25	76	73	−77	
II	11, 0, −153	−43, −11, 8	75	69	−116	
$\mathbf{h}_3^{(2)}$ $I_{||}$	4, 63, −154	(−49, 42, −26)/(−60, 45, −23)	80	81	−78	−205
$I_<$	3, 17, −107	(−48, 41, −25)/(−57, −50, −30)	81	76	−78	−157
$\mathbf{h}_3^{(1)}$ I	8, 60, −117	−52, 46, −28	73	68	−79	
II	13, 29, −180	−43, −11, 9	76	72	−115	
h I	11, 57, −163	−47, 32, −22	72	68	−104	
II[a]	13, 25, −175	−42, −4, 5	77	72	−114	

Notations: θ_X,ψ_X,φ_X – Euler angles of OEG (X = E) and amide group (X = N), angles for lower (l) and upper (u) amides are slashed as l/u; $\tau_{l(u)}$ – dihedral angle of lower (upper) OCCO group; τ_{CNCC} and τ_{OCCN} denote CNCC and OCCN dihedrals, respectively.
[a] [28].

Table 2
DFT calculated parameters of one- and two-layer networks of hydrogen bonding in model SAMs with buried amide-OEG ($\mathbf{h}_{3,6}^{(1)}$, h) and amide-OEG-amide ($\mathbf{h}_{3,6}^{(2)}$) modules.

Notation	Optimized values									
	$\mathbf{h}_6^{(2)}$		$\mathbf{h}_6^{(1)}$		$\mathbf{h}_3^{(2)}$		$\mathbf{h}_3^{(1)}$		h	
	$I_{\|\|}$	$II_<$	I	II	$I_{\|\|}$	$I_<$	I	II	I	II
$\gamma_{C=O}$	83/81	81/81	83	81	83/76	83/80	82	81	82	81
γ_{C-N} ($=\theta_N$)	−49/−54	−43/−54	−48	−43	−49/−60	−48/−57	−52	−43	−47	−42
γ_{N-H}	101/103	103/103	101	103	101/108	101/104	102	103	102	103
$\gamma_{H\cdots O}$	73/79	73/79	73	73	73/89	73/81	76	73	74	72
∠(N–H···O)	173/176	177/176	173	177	173/157	173/174	174	177	176	175
∠(H···O,H···O)	15	65	–		17	68	–		–	
d(H···O), Å	1.90/1.85	1.89/1.86	1.90	1.89	1.90/1.76	1.90/1.81	1.85	1.89	1.90	1.91
ΔE_{tot}, kcal/mol	33.3	33.8	24.3	24.2	31.3	32.8	20.2	18.4	20.0	18.6

Notations: γ_{X-Y} – angle between z axis bond X—Y=C=O, C–N, N–H; ∠(N–H···O) – angle between N–H and H···O bonds within HBA chains; ∠(H···O,H···O) angle between H···O bonds of lower and upper HBA chains; d(H···O) – length of hydrogen bonds. Values of γ_{X-Y}, ∠(N–H···O), and d(H···O) for the lower and upper HBAs are slashed as l/u; ΔE_{tot} – difference between the energy per molecule in the optimized array and the SCF energy value of isolated molecule with the same geometry.

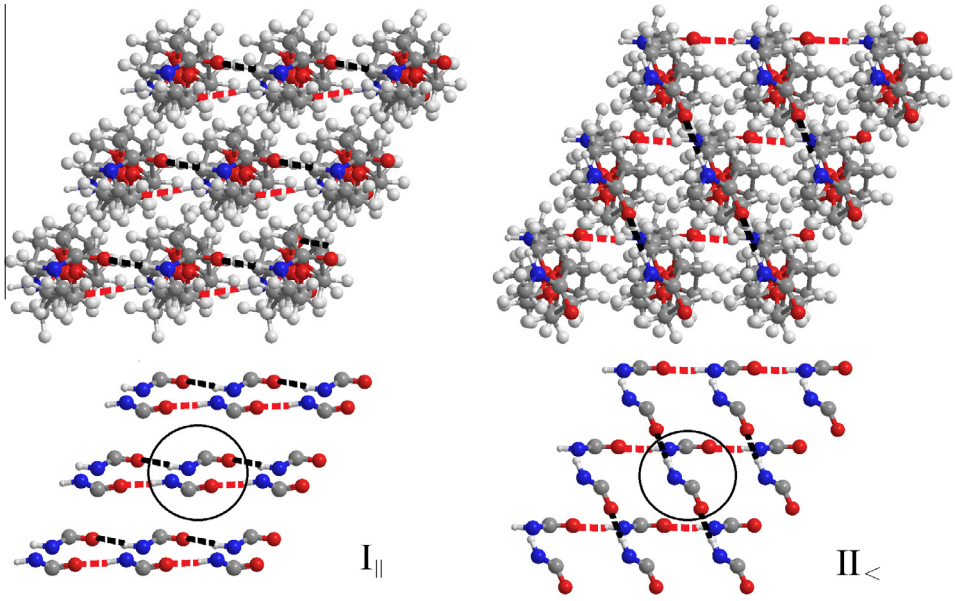

Figure 3. Top view of a 3 × 3 fragment of array $\mathbf{h}_6^{(2)}$ in different conformations (upper panels) and corresponding networks of hydrogen bonding with parallel and crossed HBA chains (lower panels). Lower (upper) H···O bonds are shown in red (black). Circles surround the lower and upper amide groups of the central molecule in the fragment. (For interpretation of the references to colour in this figure legend, the reader is referred to the web version of this article.)

It is noteworthy that the single-molecule modeling does not predict the formation of hydrogen bonding network with crossed HBA chains in SAMs containing module $A(EG)_6C_1A$. This is predetermined by the orientation of the upper and lower amide groups in the optimized geometry of molecule M2. When passing from conformation state I to II in array $\mathbf{h}_6^{(2)}$, the upper H···O bond turns clockwise giving conformation $II_<$, for which the angle between upper and lower chains equals 60°. Our observations regarding arrays of $A(EG)_3C_1A$ modules are quite different. In this case, a similar single molecule modeling does not tell us which of possible angles between the upper and lower HBA chains is preferable. *Ab initio* calculations has shown that the parallel, as well as crossed under ±60° orientation is nearly equally probable. Represented in Table 1 conformation $I_<$ of $\mathbf{h}_3^{(2)}$ corresponds to 60° clockwise turn of the upper HBA chain with respect to the lower.

In the hydrogen bonding networks with parallel and crossed HBA chains, each module $A(EG)_6C_1A$ is linked with respectively *two* and *four* nearest neighbors by *double* and *single* hydrogen bonds. This implies different deformation properties and very likely, an improved stability of SAMs with crossed HBA chains.

4. Conclusion

We have identified the optimized geometries of $(\sqrt{3} \times \sqrt{3})$ R30° hexagonal periodic arrays of OEG- and amide-containing molecular modules which can form one- and two-layered hydrogen-bonding networks in the respective families of SAMs. The networks are quantified in terms of bond–bond and bond–z-axis angles, as well as amide and OEG-related dihedral angles. The characteristic angles $\gamma_{C=O}$, γ_{N-H} and γ_{C-N} which determine the apparent intensity of amide I, III, and II bands, are shown to be ∼80°, ∼100° and ∼45–60°, respectively. These angles ensure the dominance of the amide II band in the IR RA spectra for SAMs on metal surfaces.

Our modeling shows that the formation of a two-layered hydrogen-bonding network due to the presence of the $A(EG)_{3,6}C_1A$ modules requires far more radical changes of the molecular conformation and orientation, than for SAMs containing $A(EG)_{3,6}$ modules with only one amide group. The conformation and orientation changes are expected to be substantially different for SAMs with shorter and longer OEG portions. In contrast, parameters of hydrogen-bonded amides within arrays of $A(EG)_3C_1A$ and $A(EG)_6C_1A$ are shown to be nearly the same, demonstrating a surprising ability of

oligo(ethylene glycols) to adopt a suitable conformation which to a large extent is dictated by the formation of three dimensional network of hydrogen bonds. The calculated energy gain associated with hydrogen bonding is ~10 kcal/mol per amide group. This value correlates very well with the difference in total energy ΔE_{tot} between the isolated and aggregated array constituents. Importantly, ΔE_{tot} substantially exceeds the typical calculation error. However, a really accurate estimate of this energy requires a much larger basis set.

Summarizing, the performed *ab initio* modeling shows that OEG SAMs containing two amide groups per molecular constituent can be found in the state with either parallel or crossed at 60° chains of hydrogen-bonded amides. A somewhat lower than doubled intensity of amide bands observed in IRAS experiments [26,27] indicates the dominance of the parallel configuration of hydrogen bonding with a small admixture of domains where HBA chains in the different layers are not parallel. Here, the two types of hydrogen bonding networks have received a detailed quantitative description which improves the understanding of SAM structure and vibration spectroscopy data.

Acknowledgments

We thank Prof. Bo Liedberg for reading and commenting the manuscript at its early stage. Partial financial support from the Visby program of Swedish Institute is gratefully acknowledged.

Appendix A. Supplementary data

Supplementary data associated with this article can be found, in the online version, at http://dx.doi.org/10.1016/j.cplett.2013.11.031.

References

[1] F. Schreiber, Prog. Surf. Sci. 65 (2000) 151.
[2] F. Schreiber, J. Phys.: Condens. Matter 16 (2004) R881.
[3] J.C. Love, L.A. Estroff, J.K. Kriebel, R.G. Nuzzo, G.M. Whitesides, Chem. Rev. 105 (2005) 1103.
[4] A. Vaish, M.J. Shuster, S. Cheunkar, Y.S. Singh, P.S. Weiss, A.M. Andrews, ACS Chem. Neurosci. 1 (2010) 495.
[5] K.L. Prime, G.M. Whitesides, Science 252 (1991) 1164.
[6] C. Pale-Grosdemange, E.S. Simon, K.L. Prime, G.M. Whitesides, J. Am. Chem. Soc. 113 (1991) 12.
[7] K.L. Prime, G.M. Whitesides, J. Am. Chem. Soc. 115 (1993) 10714.
[8] P. Harder, M. Grunze, R. Dahint, G.M. Whitesides, P.E. Laibinis, J. Phys. Chem. B 102 (1998) 426.
[9] J. Lahiri, L. Isaaks, J. Tien, G.M. Whitesides, Anal. Chem. 71 (1999) 777.
[10] D.J. Vanderah, H. La, J. Naff, V. Silin, K.A. Robinson, J. Am. Chem. Soc. 126 (2004) 13639.
[11] F. Zhang et al., J. Phys. Chem. A 111 (2007) 12229.
[12] C. Boozer, S. Chen, S. Jiang, Langmuir 22 (2006) 4694.
[13] R. Valiokas, S. Svedhem, S.C.T. Svensson, B. Liedberg, Langmuir 15 (1999) 3390.
[14] R. Valiokas, S. Svedhem, M. Östblom, S.C.T. Svensson, B. Liedberg, J. Phys. Chem. B 105 (2001) 5459.
[15] R. Valiokas, M. Östblom, S. Svedhem, S.C.T. Svensson, B. Liedberg, J. Phys. Chem. B 106 (2002) 10401.
[16] R.S. Clegg, J.E. Hutchison, Langmuir 12 (1996) 5239.
[17] V. Chechik, H. Schönherr, G.J. Vansco, C.J.M. Stirling, Langmuir 14 (1998) 3003.
[18] R.S. Clegg, S.M. Reed, J.E. Hutchison, J. Am. Chem. Soc. 120 (1998) 2486.
[19] R.S. Clegg, J.E. Hutchison, J. Am. Chem. Soc. 121 (1999) 5319.
[20] R.S. Clegg, S.M. Reed, R.K. Smith, B.L. Barron, J.A. Rear, J.E. Hutchison, Langmuir 15 (1999) 8876.
[21] J.H. Kim, S.S. Shin, S.B. Kim, T. Hasegawa, Langmuir 20 (2004) 1674.
[22] M.K. Ferguson, E.R. Low, J.R. Morris, Langmuir 20 (2004) 3319.
[23] L. Malysheva, Yu. Klymenko, A. Onipko, R. Valiokas, B. Liedberg, Chem. Phys. Lett. 370 (2003) 451.
[24] D. Tsankov, I. Philipova, K. Kostova, K. Hinrichs, J. Micromachines 2 (2011) 306.
[25] R. Valiokas, M. Östblom, F. Björefors, B. Liedberg, J. Shi, P. Konradsson, Biointerphases 1 (2006) 22.
[26] R. Valiokas et al., J. Electron Spectrosc. Relat. Phenom. 172 (2009) 9.
[27] H.-H. Lee et al., Langmuir 25 (2009) 13959.
[28] L. Malysheva, A. Onipko, B. Liedberg, J. Phys. Chem. A 112 (2008) 1683.
[29] C.L. Cheung, J.A. Camarero, B.W. Woods, T.W. Lin, J.E. Johnson, J.J. De Yoreo, J. Am. Chem. Soc. 125 (2003) 6848.
[30] E. Nilebäck, L. Feuz, H. Uddenberg, R. Valiokas, S. Svedhem, Biosens. Bioelectron. 28 (2011) 407.
[31] L. Zhang, W.A. Goddard, S. Jiang, J. Chem. Phys. 117 (2002) 7342.
[32] S. Vemparala, R.K. Kalia, A. Nakano, P. Vashishta, J. Chem. Phys. 121 (2004) 5427.
[33] A.J. Pertsin, M. Grunze, Langmuir 16 (2000) 8829.
[34] D. Fisher, A. Curioni, W. Andreoni, Langmuir 19 (2003) 3567.
[35] L. Malysheva, A. Onipko, R. Valiokas, B. Liedberg, J. Phys. Chem. A 109 (2005) 7788.
[36] B.I. Dunlap, J. Mol. Struct. (Theochem) 529 (2000) 37.